Engineering with Computers (2016) 32:189–206
DOI 10.1007/s00366-015-0410-5

ORIGINAL ARTICLE

Application of several non-linear prediction tools for estimating uniaxial compressive strength of granitic rocks and comparison of their performances

Danial Jahed Armaghani[1] · Edy Tonnizam Mohamad[1] · Mohsen Hajihassani[2] · Saffet Yagiz[3] · Hossein Motaghedi[4]

Received: 9 June 2015 / Accepted: 4 August 2015 / Published online: 19 August 2015
© Springer-Verlag London 2015

Abstract Uniaxial compressive strength (UCS) of rock is crucial for any type of projects constructed in/on rock mass. The test that is conducted to measure the UCS of rock is expensive, time consuming and having sample restriction. For this reason, the UCS of rock may be estimated using simple rock tests such as point load index ($I_{s(50)}$), Schmidt hammer (R_n) and p-wave velocity (V_p) tests. To estimate the UCS of granitic rock as a function of relevant rock properties like R_n, p-wave and $I_{s(50)}$, the rock cores were collected from the face of the Pahang–Selangor fresh water tunnel in Malaysia. Afterwards, 124 samples are prepared and tested in accordance with relevant standards and the dataset is obtained. Further an established dataset is used for estimating the UCS of rock via three-nonlinear prediction tools, namely non-linear multiple regression (NLMR), artificial neural network (ANN) and adaptive neuro-fuzzy inference system (ANFIS). After conducting the mentioned models, considering several performance indices including coefficient of determination (R^2), variance account for and root mean squared error and also using simple ranking procedure, the models were examined and the best prediction model was selected. It is concluded that the R^2 equal to 0.951 for testing dataset suggests the superiority of the ANFIS model, while these values are 0.651 and 0.886 for NLMR and ANN techniques, respectively. The results pointed out that the ANFIS model can be used for predicting UCS of rocks with higher capacity in comparison with others. However, the developed model may be useful at a preliminary stage of design; it should be used with caution and only for the specified rock types.

Keywords Uniaxial compressive strength · Granite · Non-linear multiple regression · Artificial neural network · Adaptive neuro-fuzzy inference system

✉ Danial Jahed Armaghani
danialarmaghani@gmail.com

Edy Tonnizam Mohamad
edy@utm.my

Mohsen Hajihassani
mohsen_hajihassani@yahoo.com

Saffet Yagiz
syagiz@pau.edu.tr

Hossein Motaghedi
hossein.motaghedi@yahoo.com

[1] Department of Geotechnics and Transportation, Faculty of Civil Engineering, Universiti Teknologi Malaysia (UTM), 81310 Skudai, Johor, Malaysia

[2] Construction Research Alliance, Universiti Teknologi Malaysia (UTM), 81310 Skudai, Johor, Malaysia

[3] Department of Geological Engineering, Engineering Faculty, Pamukkale University, 20020 Denizli, Turkey

[4] Department of Civil Engineering, Islamic Azad University, Qaemshahr Branch, Qaemshahr, Iran

1 Introduction

Rock strength plays a significant role in any type of geotechnical projects such as slope and tunnels. The uniaxial compressive strength (UCS) of rock may be estimated directly with standard test method suggested by ISRM (International Society for Rock Mechanics) or ASTM (American Standards for Testing Materials). However, some impeding factors, such as obtaining standard intact rock samples especially in highly jointed faulted rock, exist in determination of UCS directly. Further, performing the direct test to measure the UCS of rock is relatively expensive and time consuming as well [1–3]. Due to that, an

estimation of the UCS from simple index tests is economic and easier in present. For these purposes, several prediction methods have been developed and published in the literature [1, 4–10]. Some simple and multiple regression analysis techniques have been used for estimating the UCS of rocks [7, 11, 12].

Several researchers have been developed empirical relations to estimate UCS. New relationships between petrographical and engineering properties of granite were proposed in the study conducted by Tugrul and Zarif [4]. They used simple regression analysis to obtain the relationship between the UCS and other rock properties including sonic velocity, $I_{s(50)}$ and Brazilian tensile strength (BTS). Sharma and Singh [8] introduced empirical equations to estimate the impact strength index, slake durability index and UCS from V_p. Yagiz [13] used non-destructive test, p-wave velocity, to estimate UCS, Schmidt hardness, modulus of elasticity, water absorption and effective porosity, slake durability index, saturated and dry density of rock. He stated that there is significant relationship between UCS and p-wave velocity of rocks. D'Andrea et al. [14] suggested a linear regression model for predicting UCS using $I_{s(50)}$. Cargill and Shakoor [15] performed test on five different rocks to evaluate the correlations between UCS and the Schmidt hammer, point load, the slake durability and the Los Angeles abrasion test values. Their results indicate that there is a strong correlation between the UCS and $I_{s(50)}$. Singh and Singh [16] obtained the relationship between $I_{s(50)}$ and UCS of quartzites. Kahraman [17] developed the relationship between UCS and some rock parameters like $I_{s(50)}$, Schmidt hammer, sound velocity tests. Young and Rosenbaum [18] developed a reliable model to control the strength and deformability of sandstone using some mineralogical properties. Kahraman and Gunaydin [19] obtained some correlation between the UCS and $I_{s(50)}$ for igneous, metamorphic and sedimentary rocks via regression analysis. Further, Basu and Kamran [20] examined the point load test on schistose rocks and its applicability for estimating UCS. Singh et al. [11] tested and verified the empirical relation between point load index and UCS for some Indian rocks. Empirical relationships to estimate UCS using P-wave velocity were suggested mainly for coal measure rocks in the studies carried out by Singh and Dubey [21] and Singh et al. [22]. Basu and Aydin [23] recommended an empirical relationship between UCS and point load index for Hong Kong Granite. Sharma et al. [24] established some statistical relationship between Schmidt hammer rebound numbers with impact strength index; slake durability index and p-wave velocity. Table 1 shows some published equations to estimate the UCS of rock.

Various researchers have utilized soft computing methods to estimate UCS [10, 43–48] from some rock index properties including point load, p-wave velocity and Schmidt hammer hardness. Sarkar et al. [49] conducted artificial neural network model to predict the UCS and shear strength of different types of rocks using dynamic wave velocity, $I_{s(50)}$, slake durability index and density. Verma and Singh [50] proposed an ANFIS model for predicting p-wave velocity and they emphasized that neuro-fuzzy method shows a good potential to model complex, nonlinear and multivariate problems. Singh and Verma [51] performed a comparative analysis of intelligent algorithms to correlate strength and petrographic properties of some schistose rocks. Singh et al. [52] also published a comprehensive paper on the prediction of UCS by soft computing methods. Yagiz et al. [53] developed model to estimate uniaxial compressive strength of carbonate rock using slake durability and index properties of rocks. They stated that the slake durability index (I_{d4}), p-wave velocity, density and Schmidt hammer values of rocks may be used for estimating the UCS of rocks. Table 2 presents several recent works on the UCS prediction using soft computing techniques.

In this study, several modeling techniques have been used for estimating the uniaxial compressive strength of rocks using various rock properties including Schmidt hardness, p-wave velocity and point load index of rocks. Furthermore, developed models have been discussed and the best model has been chosen to be used for engineering practices.

2 Data source and structure

The Pahang–Selangor fresh water tunnel in Malaysia has been investigated to obtain the rock cores to gain the research goals. The tunnel that is crossed under the main mountain range between Pahang and Selangor states is constructed to transfer the fresh water from Pahang state to Selangor and Kuala Lumpur states in the Country. The tunnel is 44.6 km long with a diameter of 5.2 m and a longitudinal gradient of 1/1900. The tunnel is designed to operate under free flow conditions with the maximum 27.6 m^3/s of fresh water discharge. 35 km of the tunnel was excavated using three different tunnel boring machines (TBMs), while the remaining tunnel was excavated using the drilling and blasting method. The mentioned TBMs were used to excavate different ground conditions, i.e., mixed ground, very hard ground and blocky ground in Pahang–Selangor fresh water tunnel. Geological map of tunnel site and sampling point along the tunnel is given in Fig. 1. The geological units include granite, metamorphic and some sedimentary rocks as seen in the geological map; however, the most of the rock which is excavated with TBMs and blasting method is composed of granite. To obtain the goal of the study, geotechnical investigation is conducted along the tunnel, and 124 granite block samples were taken from

Table 1 Lists of UCS correlations and their descriptions

References	Correlation	R^2	Description
Aufmuth [25]	$UCS = 0.33(R_n\rho)^{1.35}$	0.80	25 different lithologies
Singh et al. [26]	$UCS = 2R_n$	0.86	Sandstone, siltstone, mudstone, seatearth
Sachpazis [27]	$UCS = 4.29R_n - 67.52$	0.96	33 different carbonates
Xu et al. [28]	$UCS = 2.98e^{(0.06R_n)}$	0.95	Mica-schist
Tugrul and Zarif [4]	$UCS = 8.36R_n - 416$	0.87	Granite
Yasar and Erdogan [29]	$UCS = 0.000004R_n^{4.29}$	0.89	Carbonates, sandstone, basalt
Kilic and Teymen [30]	$UCS = 0.0137R_n^{.2721}$	0.93	Different rock types
Yagiz [9]	$UCS = 0.0028R_n^{2.584}$	0.85	9 different rock types
Kahraman [17]	$UCS = 8.41I_{s(50)} + 9.51$	0.72	27 different rock samples
Sulukcu and Ulusay [31]	$UCS = 15.31I_{s(50)}$	0.64	23 samples in different rock types
Tsiambaos and Sabatakakis [32]	$UCS = 7.3I_{s(50)}^{1.71}$	0.82	188 samples (limestone, sandstone and marlstones)
Kahraman et al. [7]	$UCS = 10.22I_{s(50)} + 24.31$	0.75	38 different rock samples
Basu and Aydin [23]	$UCS = 18I_{s(50)}$	0.97	40 granitic rock samples
Yilmaz and Yuksek [33]	$UCS = 12.4I_{s(50)} - 9.0859$	0.81	39 gypsum sample sets
Diamantis et al. [34]	$UCS = 19.79I_{s(50)}$	0.74	32 samples of serpentinite rock
Mishra and Basu [35]	$UCS = 14.63I_{s(50)}$	0.88	60 samples (granite, schist and sandstone)
Kohno and Maeda [36]	$UCS = 16.4I_{s(50)}$	0.85	44 different rock samples
Kahraman [3]	$UCS = 2.68e^{0.93I_{s(50)}}$	0.86	32 samples of pyroclastic rocks
Sharma and Singh [8]	$UCS = 0.0642V_p - 117.99$	0.90	49 samples in different rock types
Kahraman [17]	$UCS = 9.95V_p^{1.21}$	0.69	27 different rock samples
Yasar and Erdogan [29]	$V_p = 0.0317UCS + 2.0195$	0.64	13 samples of various carbonate rock types
Moradian and Behnia [37]	$UCS = 165.05\exp(-4.452/V_p)$	0.70	64 different rock samples
Khandelwal [38]	$UCS = 0.033V_p - 34.83$	0.87	12 samples of a wide rock types
Khandelwal and Singh [39]	$UCS = 0.1333V_p - 227.19$	0.96	12 different rock samples
Minaeian and Ahangari [2]	$UCS = 0.005V_p$	0.94	Some samples of weak conglomeratic rock
Diamantis et al. [34]	$UCS = 0.11V_p - 515.56$	0.81	32 samples of serpentinite rock
Entwisle et al. [40]	$UCS = 0.78e^{0.88V_p}$	0.53	171 samples of Volcanic rock
Yagiz [13]	$UCS = 0.258V_p^{3.543}$	0.85	9 types of rock
Tonnizam Mohamad et al. [41]	$UCS = 0.032V_p - 44.23$	0.83	40 samples of soft rocks
Jahed Armaghani et al. [42]	$UCS = 0.0308V_p - 61.61$	0.47	45 samples of granitic rocks

R_n Schmidt hammer rebound no., $I_{s(50)}$ point load test, V_p p-wave velocity, ρ density of the rock

the face of the tunnel in different TBMs site to perform the planned rock testing program. These blocks were taken to the laboratory and the samples were prepared according to the International Society for Rock Mechanics [64]. In this study, representative rock blocks having no defect and discontinuities were collected from site to conduct laboratory tests as much as can be.

Afterwards, laboratory tests including Schmidt hammer rebound number (R_n), point load index ($I_{s(50)}$), p-wave velocity (V_p) and UCS were carried out on those samples. If the samples were failed along the fractures or any defects, then this test result was extracted and not counted in the dataset since it may not characterize the intact rock strength. Results of the laboratory tests conducted in this study are shown in Table 3. As a result, the established datasets have been used for developing several models by performing different techniques and, then, introduced models are compared to each other for choosing the best model among them.

3 Model constructions

To predict the uniaxial compressive strength of rocks, several methods including simple regression, non-linear multiple regression (NLMR), artificial neural network (ANN) and adaptive neuro-fuzzy inference system (ANFIS) have been utilized herein. The following sections describe modeling procedure of the aforementioned methods to predict the UCS of intact rock like granite. For this purpose, developed data set including R_n, $I_{s(50)}$, and V_p for 124 samples is used as inputs for purposed models. Afterward, estimated

Table 2 Recent works on UCS prediction using soft computing techniques

Reference	Technique	Input	R^2
Meulenkamp and Grima [54]	ANN	L, n, ρ, d	0.95
Gokceoglu and Zorlu [1]	FIS	$I_{s(50)}$, BPI, V_p, BTS	0.67
Zorlu et al. [55]	ANN	q, ρ, d, cc	0.76
Yilmaz and Yuksek [33]	ANN	n_e, $I_{s(50)}$, R_n, I_d	0.93
Yilmaz and Yuksek [56]	ANFIS	V_p, $I_{s(50)}$, R_n, W_c	0.94
Dehghan et al. [48]	ANN	V_p, $I_{s(50)}$, R_n, n	0.86
Rabbani et al. [57]	ANN	n, BD, S_w	0.96
Rezaei et al. [58]	FIS	R_n, ρ, n	0.95
Ceryan et al. [59]	ANN	I_d, V_p, n_e, PSV	0.88
Yagiz et al. [53]	ANN	V_p, n, R_n, ρ, I_d	0.50
Beiki et al. [60]	GA	ρ, n, V_p	0.83
Yesiloglu-Gultekin et al. [10]	ANFIS	BTS, V_p	0.68
Mishra and Basu [61]	FIS	V_p, $I_{s(50)}$, R_n, BPI	0.98
Torabi-Kaveh et al. [62]	ANN	V_p, ρ, n	0.95
Tonnizam Mohamad et al. [41]	ANN-PSO	BD, V_p, $I_{s(50)}$, BTS	0.97
Momeni et al. [63]	ANN-PSO	R_n, ρ, V_p, $I_{s(50)}$	0.97

L Equotip value, ρ density, *d* grain size, *PSV* petrography study values, *BPI* block punch index, *BD* bulk density, S_w water saturation, I_d slake durability index, V_p p-wave velocity, n_e effective porosity, *q* quartz content, W_c water content, *GA* genetic algorithm, *n* porosity, $I_{s(50)}$ point load, *cc* concavo convex, *PSO* particle swarm optimization

UCS values are compared with actual UCS values obtained from laboratory study.

3.1 Simple regression model and input selection

In this study, first of all, simple regression analyses were conducted to examine the weight of each parameter as input for purposed models. Relevant rock properties that were measured in the laboratory were analyzed to obtain new empirical relations to predict the UCS. In this regard, some equation types such as linear, exponential, power and logarithmic were examined for each predictor as tabulated in Table 4. In this table, values of R^2 were considered to evaluate the capacity performances of the developed empirical equations. In addition, selected equations for each predictor model are highlighted. As result, the best relationship was obtained as exponential, linear and power between the UCS and other rock properties including R_n, $I_{s(50)}$, and V_p, respectively. The obtained relationships between measured variables and the UCS of rock are given in Figs. 2, 3 and 4. The results revealed that the relationships between the relevant variables and the UCS are statistically meaningful and acceptable. Although gained results are relatively acceptable for predicting UCS, the multiple linear regression analysis was also performed to obtain the best estimation.

3.2 Non-linear multiple regression model

Multiple regression techniques can be applied to obtain the best-fit equation when more than one input parameter was needed. In common, the objective of this estimation method is to develop a relationship between more than one inputs and outputs. There are two types of multiple regressions, namely linear and non-linear. Using linear multiple regression (LMR) technique, a linear relationship can be achieved between inputs and output parameters, while non-linear multiple regression (NLMR) is an approach to obtain a non-linear relationship between relevant parameters. Many researchers proposed both NLMR and LMR equations for predicting UCS of rock using different rock index properties [1, 10, 42, 48, 65, 66]. In the present study, considering the simple regression analysis, the NLMR equations were introduced and the process was performed via iteration algorithm. The NLMR models were constructed using statistical software package of SPSS version 16 [67] herein. For this purpose, all datasets were normalized using the following equation:

$$X_{\text{norm}} = (X - X_{\text{min}})/(X_{\text{max}} - X_{\text{min}}) \quad (1)$$

where X_{min} is the minimum value of the measured parameter, X_{max} is the maximum value of the measured parameter, X and X_{norm} are the measured and normalized values in the dataset, respectively. Furthermore, five different datasets were selected randomly for training and testing to develop non-linear models.

The idea behind using some datasets for testing is to check the performance capacity of each model to select the best one. Swingler [68] and Looney [69] suggested that the 20 and 25 % of the all datasets can be used for testing. Also, Nelson and Illingworth [70] stated that the 20 to 30 % of the whole datasets may be used for testing. Considering these suggestions in the literature, 20 % of the database was selected randomly for testing, whereas the remaining 80 % of data were used for training the constructed models. Random data selection for purposed models was performed utilizing the ANN code written by authors. Using the constructed datasets, five NLMR equations have been proposed as listed in Table 5. In these models, Schmidt hardness, point load index and p-wave velocity parameters were utilized as inputs and then the UCS of rock was estimated as function of the mentioned rock properties. While the regression coefficients (R^2) of training dataset that used for modeling were various from 0.747 and 0.789, testing datasets have regression coefficients ranges from 0.471 to 0.706 as in Table 5.

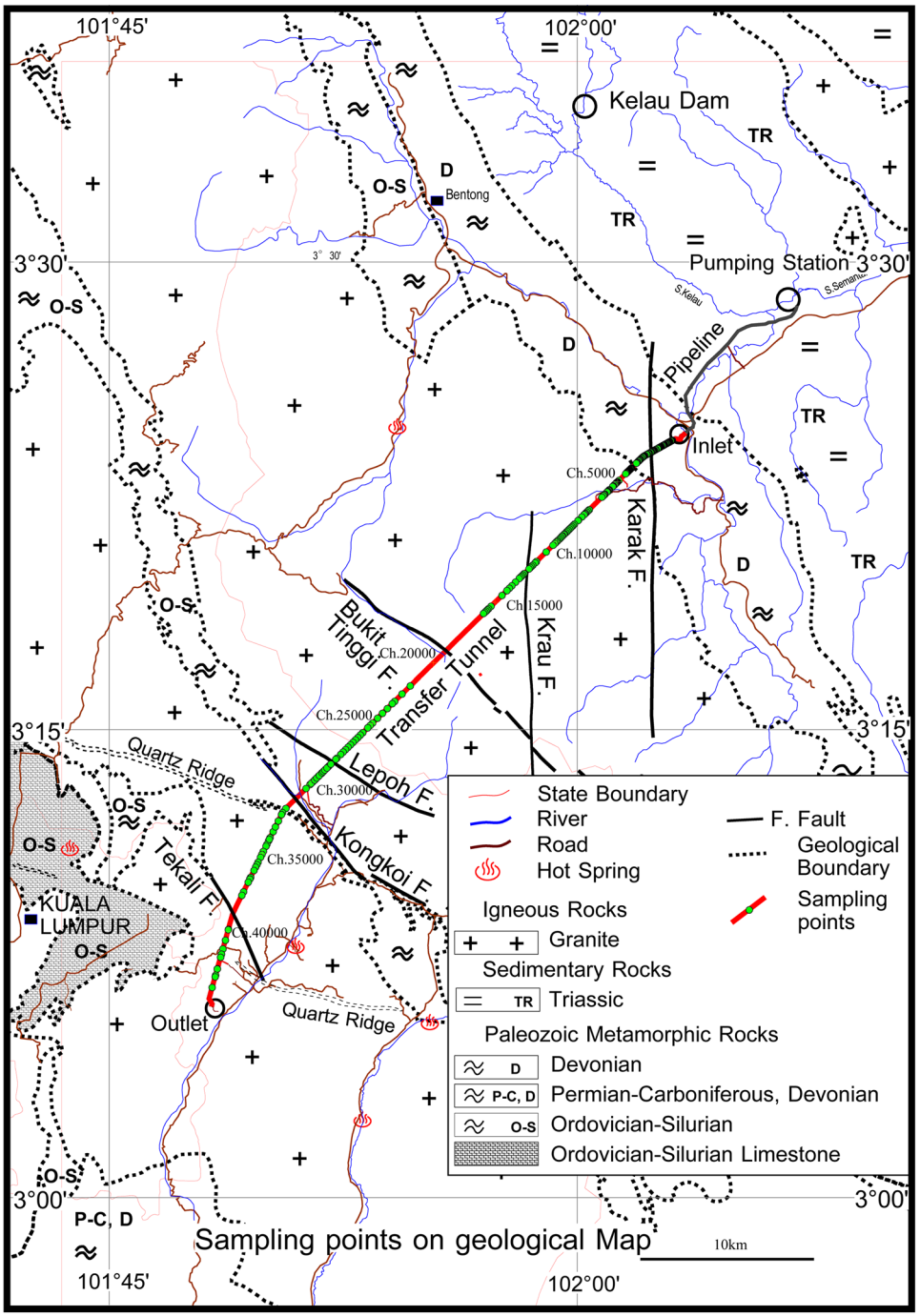

Fig. 1 Geological map around the tunnel

3.3 ANN model

Artificial neural network (ANN) is a soft computing technique inspired by the human-brain information process. A typical ANN consists of three main constituents, namely learning rule, network architecture, and transfer function [71]. There are two major types of ANN: recurrent and feed-forward. Shahin et al. [72] stated that if there is no time-dependent parameter in the ANN, the feed-forward (FF) ANN can be employed. The multi-layer perceptron (MLP) neural network is one of the most well-known FF-ANNs [73]. MLP consists of several nodes or neurons in three layers (input, hidden and output) linked to each other by weights. Du et al. [74] and Kalinli et al. [75] reported on the high efficiency of MLP-ANNs in approximating various functions in high-dimensional spaces. Nevertheless, the ANN needs to be trained before interpreting the results. Among many kinds of learning algorithms to train MLP-FF, the back-propagation (BP) is the most extensively utilized algorithm (Dreyfus, 2005). In a BP-ANN,

Table 3 Results of laboratory tests conducted in this study

Dataset no.	Rock type	Weathering zone	R_n	V_p (m/s)	$I_{s(50)}$ (MPa)	UCS (MPa)
1	Granite	Fresh	40	5506	2.31	82.6
2	Granite	Slightly weathered	39	6450	2.87	75.0
3	Granite	Slightly weathered	37	3050	3.89	62.9
4	Granite	Slightly weathered	45	2920	1.82	55.4
5	Granite	Fresh	48	5950	3.12	132.9
6	Granite	Fresh	55	3780	2.4	87.9
7	Granite	Slightly weathered	34	3102	4.56	77.9
8	Granite	Slightly weathered	33	3020	3.01	64.2
9	Granite	Slightly weathered	35	6910	2.1	69.9
10	Granite	Fresh	50	5217	3.22	97.9
11	Granite	Fresh	26	3525	1.73	89.8
12	Granite	Slightly weathered	35	2910	3.79	59.6
13	Granite	Fresh	42	4670	3.34	102.9
14	Granite	Slightly weathered	44	5345	1.93	111.9
15	Granite	Slightly weathered	27	6190	3.14	81.3
16	Granite	Fresh	36	4568	2.45	96.7
17	Granite	Slightly weathered	22	5785	1.98	71.9
18	Granite	Slightly weathered	50	7002	4.97	89.7
19	Granite	Slightly weathered	32	6790	2.59	89.5
20	Granite	Fresh	38	5310	3.96	100.8
21	Granite	Fresh	42	6635	2.02	105.7
22	Granite	Moderately weathered	23	3303	3.12	58.6
23	Granite	Moderately weathered	20	3608	2.51	48.8
24	Granite	Moderately weathered	28	3080	3.23	56.8
25	Granite	Slightly weathered	40	3620	3.21	65.7
26	Granite	Slightly weathered	41	3520	1.41	52.5
27	Granite	Moderately weathered	42	3520	2.89	51.5
28	Granite	Moderately weathered	31	3520	2.44	63.7
29	Granite	Moderately weathered	37	3010	1.56	39.0
30	Granite	Moderately weathered	34	3210	3.49	60.0
31	Granite	Moderately weathered	24	3670	1.23	44.7
32	Granite	Moderately weathered	18	3545	1.11	52.7
33	Granite	Moderately weathered	27	5643	2.75	55.6
34	Granite	Slightly weathered	45	4955	3.21	77.7
35	Granite	Slightly weathered	43	3850	2.12	84.3
36	Granite	Slightly weathered	44	3988	1.92	59.9
37	Granite	Slightly weathered	28	5040	4.65	61.2
38	Granite	Slightly weathered	27	3615	3.34	46.0
39	Granite	Moderately weathered	26	3943	1.54	40.0
40	Granite	Moderately weathered	22	4980	1.86	44.0
41	Granite	Slightly weathered	24	4080	1.21	57.0
42	Granite	Moderately weathered	41	4005	1.78	54.7
43	Granite	Moderately weathered	26	4125	2.25	42.8
44	Granite	Slightly weathered	25	3555	1.13	51.9
45	Granite	Slightly weathered	40	3430	2.99	53.2
46	Granite	Slightly weathered	37	6120	2.15	61.3
47	Granite	Moderately weathered	33	4895	3.29	72.5
48	Granite	Moderately weathered	32	4615	2.38	74.6
49	Granite	Moderately weathered	34	3715	2.88	71.5
50	Granite	Moderately weathered	40	4709	2.33	73.6

Table 3 continued

Dataset no.	Rock type	Weathering zone	R_n	V_p (m/s)	$I_{s(50)}$ (MPa)	UCS (MPa)
51	Granite	Moderately weathered	27	3301	1.02	39.4
52	Granite	Moderately weathered	19	2823	3.22	43.5
53	Granite	Moderately weathered	24	3378	3.72	48.2
54	Granite	Slightly weathered	40	4823	3.02	117.9
55	Granite	Slightly weathered	38	5065	2.91	122.3
56	Granite	Slightly weathered	48	6635	6.39	166.3
57	Granite	Slightly weathered	46	6233	3.21	138.6
58	Granite	Fresh	45	5490	4.67	124.7
59	Granite	Fresh	44	5230	3.31	110.9
60	Granite	Fresh	57	7003	5.02	152.4
61	Granite	Fresh	56	5268	2.89	106.7
62	Granite	Fresh	52	6480	5.33	180.1
63	Granite	Slightly weathered	51	6108	4.34	149.0
64	Granite	Slightly weathered	47	4250	2.78	95.6
65	Granite	Slightly weathered	49	4530	2.43	80.5
66	Granite	Slightly weathered	55	5876	3.23	121.3
67	Granite	Fresh	56	5463	3.23	107.6
68	Granite	Fresh	45	5520	3.02	101.9
69	Granite	Moderately weathered	48	5270	3.89	81.5
70	Granite	Slightly weathered	57	5109	3.67	117.9
71	Granite	Fresh	57	6659	4.89	163.3
72	Granite	Fresh	54	6148	5.89	141.7
73	Granite	Slightly weathered	45	5920	1.82	87.9
74	Granite	Fresh	49	5950	3.12	120.0
75	Granite	Fresh	52	4780	4.4	137.2
76	Granite	Moderately weathered	39	6102	2.56	93.0
77	Granite	Slightly weathered	53	5020	3.01	123.5
78	Granite	Fresh	58	6910	2.1	109.9
79	Granite	Slightly weathered	43	5217	2.22	80.3
80	Granite	Slightly weathered	46	5025	1.73	99.9
81	Granite	Slightly weathered	31	4910	3.79	88.3
82	Granite	Slightly weathered	30	4670	3.34	100.6
83	Granite	Slightly weathered	54	5345	1.93	104.3
84	Granite	Fresh	48	6190	6.14	184.9
85	Granite	Slightly weathered	55	4568	2.45	102.5
86	Granite	Slightly weathered	37	5785	1.98	114.6
87	Granite	Slightly weathered	42	7002	4.97	105.4
88	Granite	Fresh	55	7943	6.59	209.4
89	Granite	Fresh	54	7310	5.45	168.7
90	Granite	Fresh	56	6635	2.02	105.6
91	Granite	Fresh	48	6503	3.12	123.5
92	Granite	Fresh	61	7608	6.51	211.9
93	Granite	Fresh	56	6080	4.9	170.7
94	Granite	Fresh	58	6620	4.21	154.4
95	Granite	Fresh	59	6320	6.41	163.3
96	Granite	Fresh	53	5832	4.89	135.1
97	Granite	Fresh	51	4922	4.44	149.5
98	Granite	Fresh	49	6848	3.56	148.6
99	Granite	Fresh	50	5380	3.49	155.6
100	Granite	Fresh	58	7433	7.1	191.7

Table 3 continued

Dataset no.	Rock type	Weathering zone	R_n	V_p (m/s)	$I_{s(50)}$ (MPa)	UCS (MPa)
101	Granite	Fresh	56	5545	5.11	178.9
102	Granite	Fresh	54	5643	2.75	100.9
103	Granite	Fresh	58	4955	3.21	152.1
104	Granite	Fresh	51	7850	5.12	141.7
105	Granite	Fresh	57	5988	4.92	143.9
106	Granite	Fresh	55	5040	5.65	159.9
107	Granite	Moderately weathered	40	4615	1.34	48.0
108	Granite	Moderately weathered	37	3943	2.54	63.8
109	Granite	Slightly weathered	30	5980	1.86	58.0
110	Granite	Moderately weathered	40	3180	0.89	40.0
111	Granite	Slightly weathered	30	6005	1.78	50.2
112	Granite	Slightly weathered	31	4125	2.25	53.6
113	Granite	Slightly weathered	39	6555	1.6	74.9
114	Granite	Slightly weathered	38	6430	2.99	105.6
115	Granite	Slightly weathered	33	6120	4.15	71.5
116	Granite	Moderately weathered	34	4895	1.29	56.5
117	Granite	Slightly weathered	44	6615	3.38	96.0
118	Granite	Moderately weathered	51	5715	4.88	87.4
119	Granite	Moderately weathered	33	6080	3.21	95.2
120	Granite	Moderately weathered	37	6005	4.78	116.8
121	Granite	Moderately weathered	33	5125	2.25	107.0
122	Granite	Slightly weathered	49	6555	2.13	105.7
123	Granite	Slightly weathered	53	6430	2.99	106.8
124	Granite	Moderately weathered	23	6120	4.15	82.2

Table 4 Results of simple regression analyses for prediction of UCS

Regression model	Predictor	Regression function	R^2
Linear	R_n	$UCS = 2.791R_n - 18.963$	0.566
	$I_{s(50)}$	$UCS = 22.115I_{s(50)} + 26.258$	0.542
	V_p	$UCS = 0.0218V_p - 15.421$	0.457
Exponential	R_n	$UCS = 25.952e^{0.030R_n}$	0.587
	$I_{s(50)}$	$UCS = 44.592e^{0.215I_{s(50)}}$	0.474
	V_p	$UCS = 26.449e^{0.0003V_p}$	0.488
Power	R_n	$UCS = 1.596R_n^{1.0898}$	0.555
	$I_{s(50)}$	$UCS = 43.847I_{s(50)}^{0.659}$	0.466
	V_p	$UCS = 0.005V_p^{1.141}$	0.494
Logarithmic	R_n	$UCS = 100.98 \ln(R_n) - 275.370$	0.517
	$I_{s(50)}$	$UCS = 64.284 \ln(I_{s(50)}) + 28.193$	0.481
	V_p	$UCS = 103.980 \ln(V_p) - 788.890$	0.445

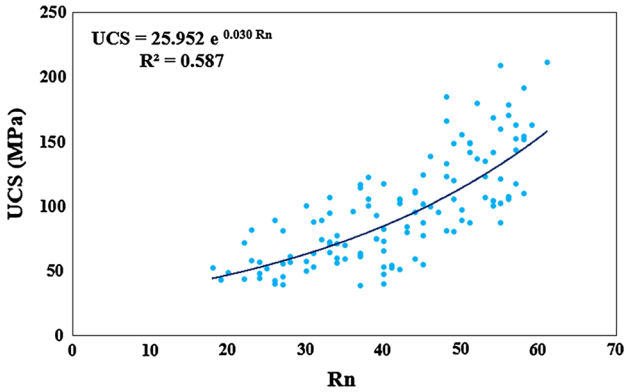

Fig. 2 Proposed equation for UCS prediction using Schmidt hammer rebound number

the imported data in the input layer start to propagate to hidden neurons through connection weights [76]. The input from each neuron in the previous layer, I_i, is multiplied by an adjustable connection or weight, W_{ij}. At each node, the sum of the weighted input signals is computed and then this value is added to a threshold value known as the bias value, B_{ij} (Eq. 2). To create the output of the neuron, the combined input, J_i, is passed through a non-linear transfer function $f(J_j)$, such as a sigmoidal function (Eq. 3). However, in general, the output of each neuron provides the input to the next layer neuron. This procedure is continued until the output is generated. To achieve the error, the created output is checked against the desired output. The BP training can change the weights between the neurons iteratively in a way that minimizes the root mean square error (RMSE) of the system. More details of the BP

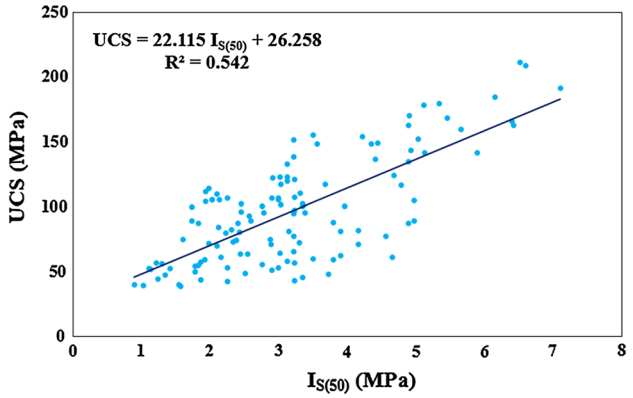

Fig. 3 Proposed equation for UCS prediction using point load index

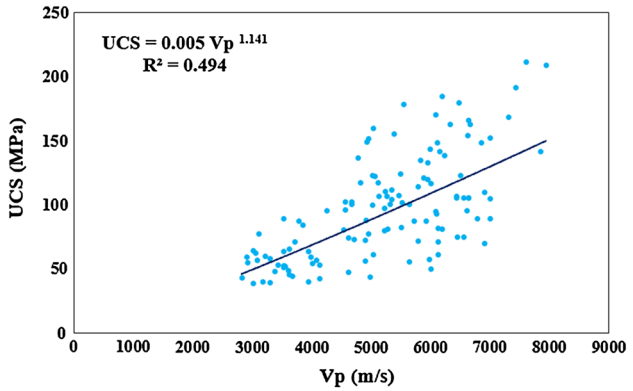

Fig. 4 Proposed equation for UCS prediction using p-wave velocity

algorithm can be seen in the classic artificial intelligence books [77].

$$J_j = \sum (w_{ij} I_i) + B_j \tag{2}$$

$$y_i = f(J_j) \tag{3}$$

In ANN modeling procedure, the same datasets of the NLMR analyses were utilized. The parameters of ANN such as momentum coefficient and learning rate play an important role in the performance capacity of the ANN models. A brief review of the previous studies is required to determine the values of these parameters. If the selected learning rate is small, the training rate will be slow. Because minor changes to weights can be occurred when small values of learning rate are implemented [6, 78]. In addition, fluctuations may happen in the results of training phase caused using large values of learning rate [6, 65]. Different learning rate values have been proposed by several authors. Learning rates of 0.05 and 0.5 were suggested in the studies conducted by Jahed Armaghani et al. [42] and Choobbasti et al. [79], respectively. Yilmaz and Yuksek [56], Erzin and Cetin [80] and Momeni et al. [81] recommended the value of 0.01 for learning rate, while this value was suggested as 0.1 in the study conducted by Yagiz et al. [65]. Apart from learning rate, a steadying effect can be observed by momentum coefficient [82]. Various values have been recommended for momentum coefficient such as 0.95 by Yagiz et al. [65], 0.9 by Jahed Armaghani et al. [42], 0.0–1.0 by Hassoun [83] and Fu [84], 0.4–0.9 by Wyhthoff [85] and close to 1.0 by Henseler [86]. According to the above discussion, it seems that different values of learning rates and the momentum coefficients can be utilized to solve the engineering problems. To determine the proper learning rate and momentum coefficient, a series of sensitivity analyses were performed in this study. Considering the provided information by various researchers and the trial-and-error procedure performed in this study, values of 0.05 and 0.9 were chosen for learning rate and the momentum coefficient, respectively.

Besides, performance of ANN models also depends strongly on the suggested architecture of the network as mentioned in the studies conducted by Hush [87] and Kanellopoulas and Wilkinson [88]. Therefore, determination of the optimal architecture is required to design an ANN model. The network architecture is defined as the number of hidden layer(s) and the number of nodes in each hidden layer(s). According to various researchers (e.g., [89–91]) and considering the results of several studies (e.g., [92, 93]), one hidden layer can solve any complex function in a network. Hence, one hidden layer was chosen to construct the ANN models. In addition, determining

Table 5 NLMR equations for five randomly selected datasets

Dataset no.	Proposed equation	R^2
1	$\mathrm{UCS} = 11.558e^{0.0301R_n} + 0.0006V_p^{1.193} + 21.938I_{s(50)} - 34.728$	0.747
2	$\mathrm{UCS} = 11.442e^{0.0297R_n} + 0.001V_p^{1.178} + 22.297I_{s(50)} - 35.051$	0.766
3	$\mathrm{UCS} = 11.707e^{0.0297R_n} + 0.001V_p^{1.1702} + 22.629I_{s(50)} - 36.986$	0.771
4	$\mathrm{UCS} = 10.817e^{0.0311R_n} + 0.0005V_p^{1.242} + 23.274I_{s(50)} - 36.567$	0.789
5	$\mathrm{UCS} = 11.506e^{0.0287R_n} + 0.001V_p^{1.196} + 21.943I_{s(50)} - 31.365$	0.757

Table 6 The proposed equations for number of neurons in hidden layer

Heuristic	References
$\leq 2 \times N_i + 1$	Hecht-Nielsen [89]
$(N_i + N_o)/2$	Ripley [95]
$\frac{2+N_o \times N_i + 0.5N_o \times (N_o^2 + N_i) - 3}{N_i + N_o}$	Paola [96]
$2N_i/3$	Wang [97]
$\sqrt{N_i \times N_o}$	Masters [98]
$2N_i$	Kaastra and Boyd [99], Kannellopoulas and Wilkinson [88]

N_i number of input neuron, N_o number of output neuron

neuron number(s) in the hidden layer is the most critical task of the ANN architecture as highlighted in the studies conducted by Sonmez et al. [6] and Sonmez and Gokceoglu [94]. Table 6 presents some proposed equations for determination of number of neuron by several scholars. As mentioned earlier, R_n, $I_{s(50)}$, and V_p were used as input parameters in the analyses of this study. Based on Table 6, considering three neurons in input layer (N_i) and one neuron in output layer (N_o), the numbers of neurons that should be used in the hidden layer are in the range of 1 and 7.

To determine the optimum number of neurons in the hidden layer, using 5 randomly selected datasets, 35 ANN models were constructed using one hidden layer and number of hidden neurons of 1 to 7 as shown in Table 7. According to Table 7, considering average R^2 value of both training and testing datasets, model no. 5 with hidden neurons of 5 outperforms the other models. Hence, five was selected as number of hidden neurons in constructing ANN models. It should be noted that only results of R^2 are considered as performance criteria to select the best model. Performance indices of all models with 5 hidden neurons for training and testing datasets are presented in Table 9. Suggested ANN structure in this study is illustrated in Fig. 5. More discussions regarding the selection of the best ANN model to predict UCS will be given in results and discussion section.

Table 8 ANFIS parameters and their values

ANFIS parameter	Value
Number of nodes	158
Number of linear parameters	256
Number of nonlinear parameters	24
Total number of parameters	280
Number of training data pairs	99
Number of checking data pairs	25
Number of fuzzy rules	64

3.4 ANFIS model

ANFIS was developed by Jang [100] based on the Takagi–Sugeno fuzzy inference system (FIS). ANFIS is constructed by a set of if–then fuzzy rules with proper membership functions to produce the required output from the input data. As a universal predictor, ANFIS has the capability of estimating any real continuous functions [101]. In general, an FIS is established based on five functioning blocks:

- Several if–then fuzzy rules
- A database to define the membership functions
- A decision-making element to conduct the inference operations on the rules
- A fuzzification interface to convert the inputs utilizing linguistic values
- A defuzzification interface to convert the fuzzy results into an output.

Table 7 Several ANN models with different hidden nodes

Model no.	Nodes in hidden layers	Network result											
		Iteration 1		Iteration 2		Iteration 3		Iteration 4		Iteration 5		Average	
		R^2		R^2		R^2		R^2		R^2		R^2	
		Train	Test	Train	Test	Train	Test	Train	Test	Train	Test	Train	Test
1	1	0.831	0.650	0.792	0.846	0.801	0.865	0.846	0.593	0.837	0.539	0.821	0.699
2	2	0.848	0.722	0.837	0.745	0.819	0.776	0.824	0.817	0.823	0.776	0.830	0.767
3	3	0.865	0.722	0.851	0.810	0.865	0.719	0.844	0.757	0.828	0.884	0.851	0.778
4	4	0.866	0.808	0.848	0.867	0.841	0.880	0.865	0.760	0.823	0.848	0.849	0.833
5	5	0.863	0.874	0.864	0.877	0.867	0.886	0.864	0.861	0.864	0.858	0.864	0.871
6	6	0.879	0.722	0.822	0.848	0.861	0.817	0.855	0.799	0.857	0.867	0.855	0.811
7	7	0.880	0.817	0.844	0.851	0.865	0.810	0.846	0.865	0.877	0.847	0.862	0.838

Table 9 Performance indices of each model and their rank values for all predictive approaches

Method	Model	R^2	RMSE	VAF	Rating for R^2	Rating for RMSE	Rating for VAF	Rank value
NLMR	Train 1	0.747	22.282	72.109	1	2	2	5
	Train 2	0.766	22.179	73.016	3	3	3	9
	Train 3	0.771	21.571	73.667	4	4	4	12
	Train 4	0.789	20.668	76.201	5	5	5	15
	Train 5	0.757	23.537	71.788	2	1	1	4
	Test 1	0.706	19.705	69.386	5	5	5	15
	Test 2	0.651	22.420	63.354	4	4	4	12
	Test 3	0.619	24.534	55.522	2	2	2	6
	Test 4	0.471	28.534	40.211	1	1	1	3
	Test 5	0.649	23.901	62.577	3	3	3	9
ANN	Train 1	0.863	14.947	86.318	3	3	1	7
	Train 2	0.864	14.180	86.405	4	5	3	12
	Train 3	0.867	14.408	86.602	5	4	5	14
	Train 4	0.864	15.060	86.425	4	2	4	10
	Train 5	0.864	15.034	86.403	4	3	2	9
	Test 1	0.874	15.401	87.369	3	5	4	12
	Test 2	0.877	17.868	85.663	4	2	3	9
	Test 3	0.886	16.444	87.758	5	4	5	14
	Test 4	0.861	16.458	84.172	2	3	1	6
	Test 5	0.858	18.104	84.191	1	1	2	4
ANFIS	Train 1	0.932	10.877	93.265	2	1	1	4
	Train 2	0.935	10.608	93.467	3	2	2	7
	Train 3	0.956	8.654	95.649	5	5	5	15
	Train 4	0.956	8.911	95.576	5	4	4	13
	Train 5	0.943	9.877	94.265	4	3	3	10
	Test 1	0.941	8.685	94.086	2	2	2	6
	Test 2	0.950	8.969	94.485	4	1	4	9
	Test 3	0.951	8.473	94.706	5	3	5	13
	Test 4	0.946	7.018	94.349	3	5	3	11
	Test 5	0.939	8.227	93.827	1	4	1	6

An ANFIS model offers the advantages of both ANN and FIS principles and presents all their benefits in a single framework. An adaptive ANN model involves numbers of nodes connected by directional links, where each node is designated using a node function with fixed or changeable parameters. In these networks, the ANN is employed to determine the unknown relationship between the parameters when the FIS is initialized. This process is called "adaptive". An adaptive ANN model which involves premise and consequent parts is shown in Fig. 6a, which equates to an FIS (Fig. 6b).

To describe the modeling procedure through an ANFIS model, it is supposed that the FIS under consideration is composed of two inputs (x, y) and one output (f) and the rule base includes a two fuzzy rule set "if–then" as below:

Rule I: if x is A_1 and y is B_1, then $f_1 = p_1x + q_1y + r_1$
Rule II: if x is A_2 and y is B_2, then $f_2 = p_2x + q_2y + r_2$

where p_i, q_i, and r_i are the consequent parameters to be settled. According to Jang [100] and Jang et al. [101], an ANFIS model with two inputs, one output, five layers and two rules (see Fig. 6b) can be described as follows:

Layer 1: Each node i in layer 1 produces a membership grade of a linguistic label. For instance, the node function of the ith node is:

$$Q_i^1 = \mu_{Ai}(x) = \frac{1}{1 + \left[\left(\frac{x - v_i}{\sigma_1}\right)^2\right]^{b_i}} \tag{4}$$

in which Q_i^1 and x are the membership function and input to node i, respectively. A_i is the linguistic label related to node i and σ_1, v_i, b_i are parameters that make changes in the form of the membership functions. The existing parameters in this layer are related to the premise part, as shown in Fig. 6a.

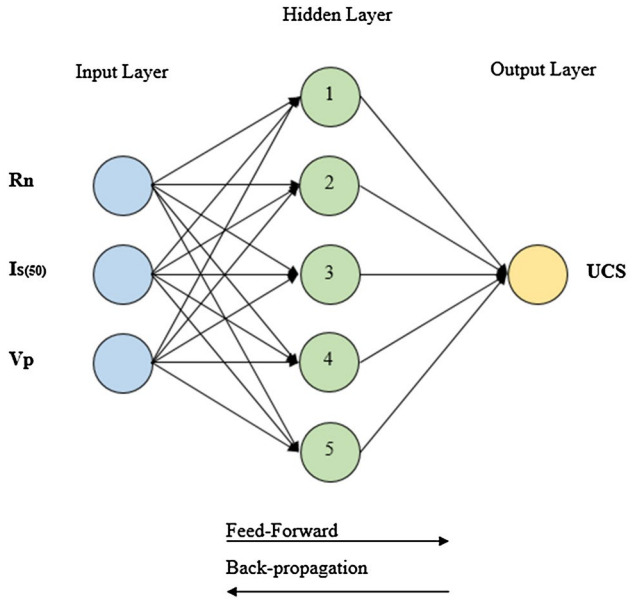

Fig. 5 Suggested structure of the ANN model

Layer 2: Each node in layer 2 computes the firing strength of each rule through multiplication:

$$Q_i^2 = w_i = \mu_{Ai}(x) \cdot \mu_{Bi}(y) \quad i = 1, 2 \tag{5}$$

Layer 3: The ratio of firing strength of the ith rule to the sum of firing strengths of all rules is obtained in this layer.

$$Q_i^3 = W_i = \frac{w_i}{\sum_{j=1}^{2} w_j} \quad i = 1, 2 \tag{6}$$

Layer 4: Every node i in this layer is a node function whereas W_i is the output of layer 3. Parameters of this layer are related to the consequent part.

$$Q_i^4 = W_i f_i = W_i(p_i x + q_i y + r_i) \tag{7}$$

Layer 5: The incoming signals are summed in this layer and form the overall output.

$$Q_i^5 = \text{Overall output} = \sum W_i f_i = \frac{\sum w_i f_i}{\sum w_i} \tag{8}$$

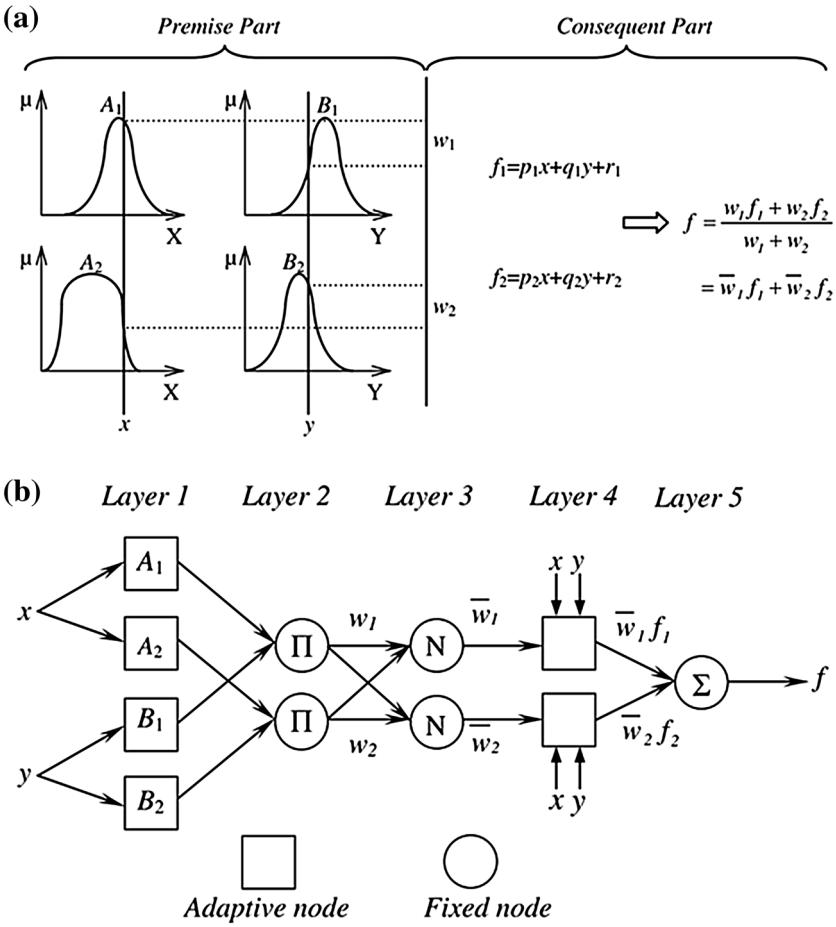

Fig. 6 **a** Sugeno fuzzy model with two rules, **b** equivalent ANFIS architecture [101]

To develop an ANFIS model for prediction of the UCS of rock, results of three index tests including R_n, $I_{s(50)}$, and V_p were utilized as input parameters. Accordingly, the results of UCS tests were set as the output parameter. The modeling was conducted over a database consisting of 124 datasets. In ANFIS technique, similar to ANN modeling, the best architecture should be determined. To this aim, using a trial-and-error procedure, several ANFIS models were constructed to determine the number of fuzzy rules. The Gaussian, as a well-known membership function in fuzzy systems, was employed for this model [42]. Eventually, each input parameter with 4 fuzzy rules outperforms the other ANFIS models. Therefore, 64 fuzzy rules ($4 \times 4 \times 4$) show the best performance for UCS prediction of the rock. In determining the number of fuzzy rules, the results of RMSE were only considered. The linguistic variables for input parameters were set to very low (VL), low (L), high (H) and very high (VH). In this step, considering the suggested ANFIS structure and using randomly selected datasets, five ANFIS models were constructed as shown in Table 9. In addition, these models were checked using the data assigned for testing datasets. Figures 7, 8 and 9 show the normalized membership functions of the input parameters for the ANFIS model. For this model, the RMSE results were not decreased after epoch number of 17. The presented membership functions were assigned after training the system. Furthermore, for the output, a linear type of membership function was utilized. Table 8 shows ANFIS parameters and their values used in the modeling. It should be mentioned that all ANN and ANFIS models in this study were constructed using MatLab version 7.14.0.739 [102].

4 Results of models performances

From simple regression results, it was found that the models with multi-input parameters may predict UCS with higher degree of accuracy. Therefore, various non-linear techniques namely NLMR, ANN and ANFIS were developed to predict UCS of rocks obtained from the face of the Pahang–Selangor fresh water tunnel in Malaysia. During the modeling process of this study, all 124 datasets were randomly selected to 5 different datasets including training

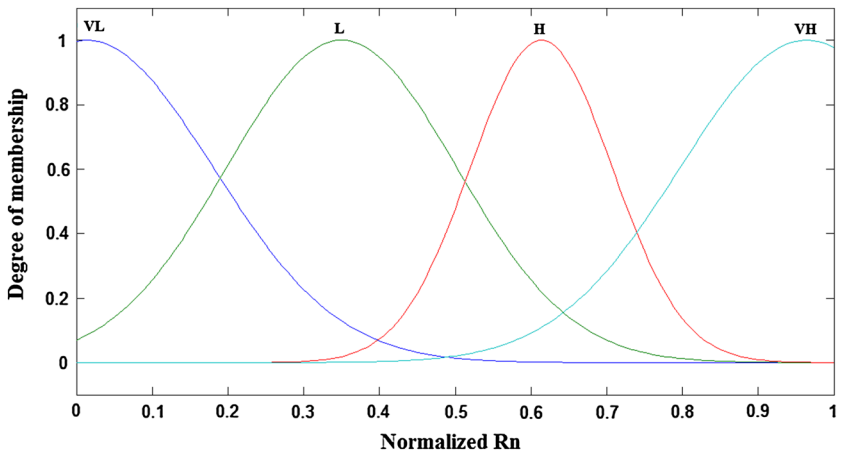

Fig. 7 Membership functions assigned for Schmidt hammer rebound number

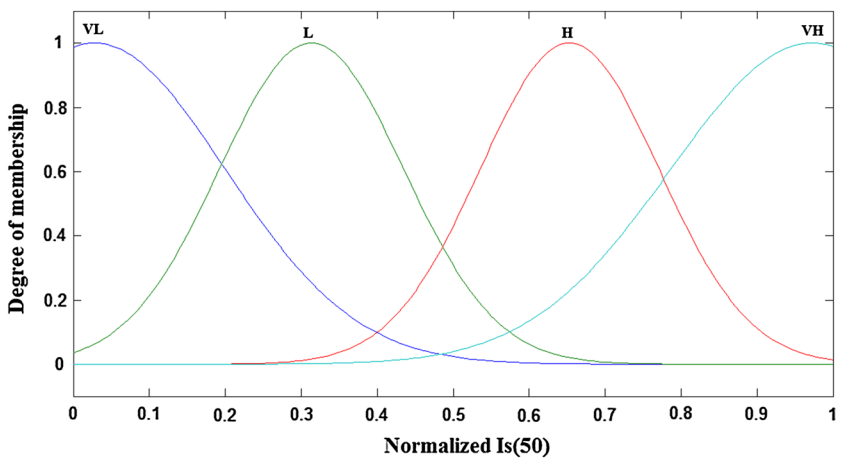

Fig. 8 Membership functions assigned for point load index

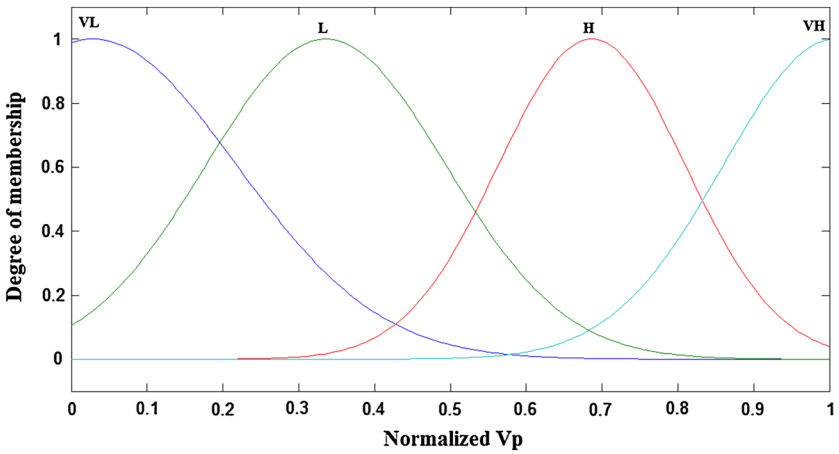

Fig. 9 Membership functions assigned for p-wave velocity

and testing for development of non-linear models. Some performance indices including R^2, variance account for (VAF) and RMSE were computed to check the capacity performance of all predictive models:

$$R^2 = 1 - \frac{\sum_{i=1}^{N}(y - y')^2}{\sum_{i=1}^{N}(y - \tilde{y})^2} \tag{9}$$

$$\text{VAF} = \left[1 - \frac{\text{var}(y - y')}{\text{var}(y)}\right] \times 100 \tag{10}$$

$$\text{RMSE} = \sqrt{\frac{1}{N}\sum_{i=1}^{N}(y - y')^2} \tag{11}$$

where y, y' and $\tilde{y}$ are the measured, predicted and mean of the y values, respectively, N is the total number of data and P is the number of predictors. Theoretically, the model will be excellent if the R^2 is one, VAF is 100 and RMSE is zero. Results of models performance indices (R^2, RMSE and VAF) for all randomly selected datasets based on training and testing are presented in Table 9. High performances of the training datasets indicate that the learning process of the predictive models is successful if those of testing datasets reveal that the models generalization ability is satisfactory. As seen in Table 9, selecting the best model for the UCS prediction is quite difficult. To overcome this difficulty, a simple ranking procedure suggested by Zorlu et al. [55] was used to select the best models. A ranking value was calculated and assigned for each training and testing dataset separately (Table 9). Total ranking of training and testing datasets for three non-linear models is shown in Table 10. According to this table, models 2 and 3 exhibited the best performances of UCS prediction for NLMR and ANN techniques, respectively, while model 3 yielded the best results among ANFIS models. When considering both training and

Table 10 Results of total rank for all predictive techniques obtained from five randomly selected datasets

Method	Model	Total rank
NLMR	1	20
	2	21
	3	18
	4	18
	5	13
ANN	1	19
	2	21
	3	28
	4	16
	5	13
ANFIS	1	10
	2	16
	3	28
	4	24
	5	16

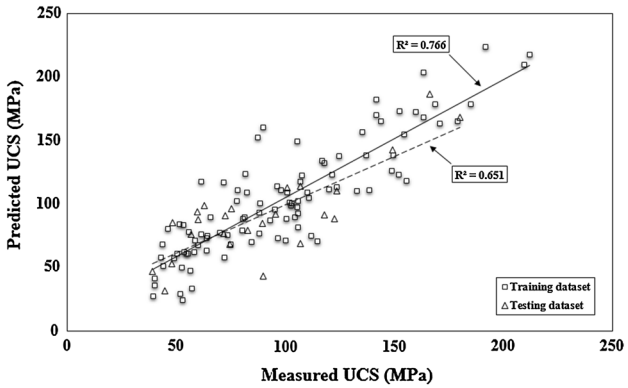

Fig. 10 R^2 of measured and predicted values of UCS for training and testing datasets using NLMR technique

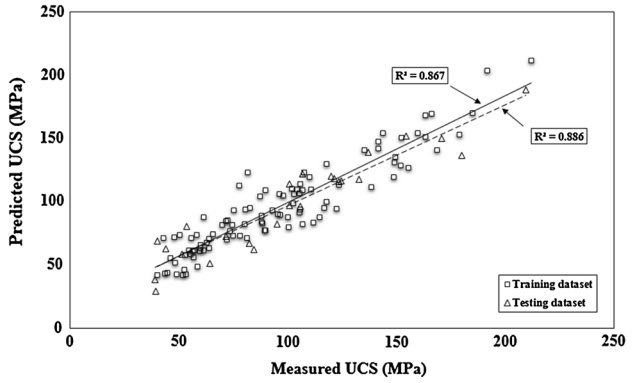

Fig. 11 R^2 of measured and predicted values of UCS for training and testing datasets using ANN technique

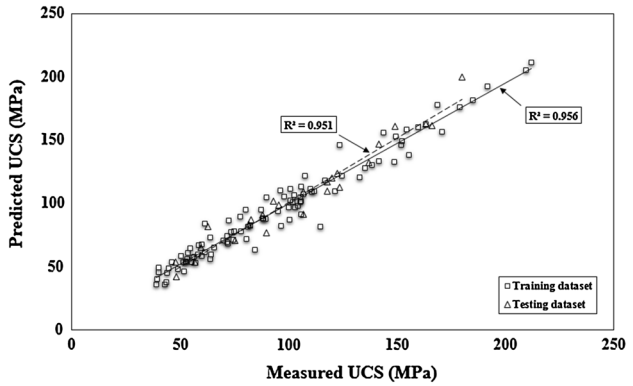

Fig. 12 R^2 of measured and predicted values of UCS for training and testing datasets using ANFIS technique

testing datasets, the prediction performances of the ANFIS models are higher than those of ANN and NLMR models. The NLMR equation for model 2 is given as follows:

$$\mathrm{UCS} = 11.442\mathrm{e}^{0.0297} R_{\mathrm{n}} + 0.001 V_{\mathrm{p}}^{1.178} + 22.297 I_{\mathrm{s}(50)} - 35.051 \quad (12)$$

Utilizing the NLMR, ANN and ANFIS methods, the developed relationship between the estimated UCS of granitic rocks and the measured one is given in Figs. 10, 11 and 12 respectively. It is shown that the best prediction model is obtained using the ANFIS technique with regression coefficient of 0.951 and 0.956 for testing and training data in comparison with others including NLMR and ANN as shown in figures.

5 Conclusions

To develop the purposed models, laboratory tests were performed on the rocks obtained from the face of the Pahang–Selangor fresh water tunnel in Malaysia herein. The dataset composed of Schmidt hammer rebound number, point load index, p-wave velocity and UCS properties of granitic rocks. Based on the dataset, several non-linear prediction models were developed for estimating the UCS of granitic rocks. The simple relationship between the UCS and input variables including R_{n}, $I_{\mathrm{s}(50)}$ and V_{p} is acceptable and obtained regression coefficients between the UCS and each variable are acceptable. Afterward, non-linear multiple regression model, the ANN and ANFIS techniques were employed for developing the best accurate predictor for estimating the UCS of rocks. Further, the developed models are compared to each other for choosing the best model one. For selecting the best model, obtained regression coefficient and total rank for each model were computed and compared. As considering the testing datasets, the prediction performance of the ANFIS models ($R^2 = 0.951$) is higher than those of the ANN model ($R^2 = 0.886$) and NLMR ($R^2 = 0.651$). Also, considering the training datasets, similar results were also obtained ($R^2 = 0.766$; 0.867; 0.956, respectively). Further, it is found that the ANFIS model gives best result in comparison with other models according to the total rank method as discussed previously. As a result, it is concluded that each developed model can be used for predicting the UCS of granitic rocks; however, the most accurate result can be obtained using the ANFIS model; however, it is obvious that developed models should be used for similar type of rocks and it is open to be developed.

Acknowledgments The authors would like to extend their sincere gratitude to the Pahang–Selangor fresh water tunnel project team, especially to Ir. Dr. Zulkeflee Nordin, Ir. Arshad, the contractor and consultant groups for facilitating this study. Further, the authors wish to express their appreciation to Universiti Teknologi Malaysia for supporting this research.

References

1. Gokceoglu C, Zorlu K (2004) A fuzzy model to predict the uniaxial compressive strength and the modulus of elasticity of a problematic rock. Eng Appl Artif Intell 17:61–72
2. Minaeian B, Ahangari K (2013) Estimation of uniaxial compressive strength based on P-wave and Schmidt hammer rebound using statistical method. Arab J Geosci 6:1925–1931
3. Kahraman S (2014) The determination of uniaxial compressive strength from point load strength for pyroclastic rocks. Eng Geol 170:33–42
4. Tugrul A, Zarif IH (1999) Correlation of mineralogical and textural characteristics with engineering properties of selected granitic rocks from Turkey. Eng Geol 51:303–317
5. Sonmez H, Tuncay E, Gokceoglu C (2004) Models to predict the uniaxial compressive strength and the modulus of elasticity for Ankara agglomerate. Int J Rock Mech Min Sci 41(5):717–729
6. Sonmez H, Gokceoglu C, Nefeslioglu HA, Kayabasi A (2006) Estimation of rock modulus: for intact rocks with an artificial neural network and for rock masses with a new empirical equation. Int J Rock Mech Min Sci 43:224–235

7. Kahraman S, Gunaydin O, Fener M (2005) The effect of porosity on the relation between uniaxial compressive strength and point load index. Int J Rock Mech Min Sci 42(4):584–589
8. Sharma PK, Singh TN (2008) A correlation between P-wave velocity, impact strength index, slake durability index and uniaxial compressive strength. Bull Eng Geol Environ 67:17–22
9. Yagiz S (2009) Predicting uniaxial compressive strength, modulus of elasticity and index properties of rocks using the Schmidt hammer. Bull Eng Geol Environ 68(1):55–63
10. Yesiloglu-Gultekin N, Gokceoglu C, Sezer EA (2013) Prediction of uniaxial compressive strength of granitic rocks by various nonlinear tools and comparison of their performances. Int J Rock Mech Min Sci 62:113–122
11. Singh TN, Kainthola A, Venkatesh A (2012) Correlation between point load index and uniaxial compressive strength for different rock types. Rock Mech Rock Eng 45:259–264
12. Monjezi M, Khoshalan HA, Razifard M (2012) A neuro-genetic network for predicting uniaxial compressive strength of rocks. Geotech Geol Eng 30(4):1053–1062
13. Yagiz S (2011) P-wave velocity test for assessment of geotechnical properties of some rock materials. Bull Mater Sci 34(4):947–953
14. D'Andrea DV, Fisher RL, Fogelson DE (1964) Prediction of compression strength from other rock properties. Colo Sch Mines Q 59(4B):623–640
15. Cargill JS, Shakoor A (1990) Evaluation of empirical methods for measuring the uniaxial compressive strength of rock. Int J Rock Mech Min Sci 27:495–503
16. Singh VK, Singh DP (1993) Correlation between point load index and compressive strength for quartzite rocks. Geotech Geol Eng 11:269–272
17. Kahraman S (2001) Evaluation of simple methods for assessing the uniaxial compressive strength of rock. Int J Rock Mech Min Sci 38:981–994
18. Young Y, Rosenbaum SM (2002) The artificial neural network as a tool for assessing geotechnical properties. Geotech Geol Eng 20:149–168
19. Kahraman S, Gunaydin O (2009) The effect of rock classes on the relation between uniaxial compressive strength and point load index. Bull Eng Geol Environ 68(3):345–353
20. Basu A, Kamran M (2010) Point load test on schistose rocks and its applicability in predicting uniaxial compressive strength. Int J Rock Mech Min Sci 47:823–828
21. Singh TN, Dubey RK (2000) A study of transmission velocity of primary wave (P-wave) in Coal Measures sandstone. J Sci Ind Res 59:482–486
22. Singh TN, Kanchan R, Saigal K, Verma AK (2004) Prediction of P-wave velocity and anisotropic properties of rock using artificial neural networks technique. J Sci Ind Res 63(1):32–38
23. Basu A, Aydin A (2006) Predicting uniaxial compressive strength by point load test: significance of cone penetration. Rock Mech Rock Eng 39(5):483–490
24. Sharma PK, Khandelwal M, Singh TN (2011) A correlation between Schmidt hammer rebound numbers with impact strength index, slake durability index and P-wave velocity. Int J Earth Sci (Geol Rundsch) 100:189–195
25. Aufmuth RE (1973) A systematic determination of engineering criteria for rocks. Bull Assoc Eng Geol 11:235–245
26. Singh RN, Hassani FP, Elkington PAS (1983) The application of strength and deformation index testing to the stability assessment of coal measures excavations. In: Proceeding of 24th US symposium on rock mechanics. Texas A and M University AEG, Balkema, Rotterdam, pp 599–609
27. Sachpazis CI (1990) Correlating Schmidt hardness with compressive strength and Young's modulus of carbonate rocks. Bull Int Assoc Eng Geol 42:75–83
28. Xu S, Grasso P, Mahtab A (1990) Use of Schmidt hammer for estimating mechanical properties of weak rock. In: Proceeding of 6th international IAEG Congress, Balkema, Rotterdam, pp 511–519
29. Yasar E, Erdogan Y (2004) Estimation of rock physiomechanical properties using hardness methods. Eng Geol 71:281–288
30. Kilic A, Teymen A (2008) Determination of mechanical properties of rocks using simple methods. Bull Eng Geol Environ 67(2):237–244
31. Sulukcu S, Ulusay R (2001) Evaluation of the block punch index test with particular reference to the size effect, failure mechanism and its effectiveness in predicting rock strength. Int J Rock Mech Min Sci 38:1091–1111
32. Tsiambaos G, Sabatakakis N (2004) Considerations on strength of intact sedimentary rocks. Eng Geol 72:261–273
33. Yilmaz I, Yuksek AG (2008) An example of artificial neural network (ANN) application for indirect estimation of rock parameters. Rock Mech Rock Eng 41(5):781–795
34. Diamantis K, Gartzos E, Migiros G (2009) Study on uniaxial compressive strength, point load strength index, dynamic and physical properties of serpentinites from Central Greece: test results and empirical relations. Eng Geol 108:199–207
35. Mishra DA, Basu A (2012) Use of the block punch test to predict the compressive and tensile strengths of rocks. Int J Rock Mech Min Sci 51:119–127
36. Kohno M, Maeda H (2012) Relationship between point load strength index and uniaxial compressive strength of hydrothermally altered soft rocks. Int J Rock Mech Min Sci 50:147–157
37. Moradian ZA, Behnia M (2009) Predicting the uniaxial compressive strength and static Young's modulus of intact sedimentary rocks using the ultrasonic test. Int J Geomech 9:1–14
38. Khandelwal M (2013) Correlating P-wave velocity with the physico-mechanical properties of different rocks. Pure Appl Geophys 170:507–514
39. Khandelwal M, Singh TN (2009) Correlating static properties of coal measures rocks with P-wave velocity. Int J Coal Geol 79:55–60
40. Entwisle DC, Hobbs RN, Jones LD, Gunn D, Raines MG (2005) The relationship between effective porosity, uniaxial compressive strength and sonic velocity of intact Borrowdale volcanic group core samples from Sella field. Geotech Geol Eng 23:793–809
41. Tonnizam Mohamad E, Jahed Armaghani D, Momeni E, Alavi Nezhad Khalil Abad SV (2014) Prediction of the unconfined compressive strength of soft rocks: a PSO-based ANN approach. Bull Eng Geol Environ. doi:10.1007/s10064-014-0638-0
42. Jahed Armaghani D, Tonnizam Mohamad E, Momeni E, Narayanasamy MS, Mohd Amin MF (2014) An adaptive neuro-fuzzy inference system for predicting unconfined compressive strength and Young's modulus: a study on Main Range granite. Bull Eng Geol Environ. doi:10.1007/s10064-014-0687-4
43. Gokceoglu C (2002) A fuzzy triangular chart to predict the uniaxial compressive strength of the Ankara agglomerates from their petrographic composition. Eng Geol 66(1–2):39–51
44. Karakus M, Tutmez B (2006) Fuzzy and multiple regression modelling for evaluation of intact rock strength based on point load, Schmidt hammer and sonic velocity. Rock Mech Rock Eng 39(1):45–57
45. Tiryaki B (2008) Predicting intact rock strength for mechanical excavation using multivariate statistics, artificial neural networks, and regression trees. Eng Geol 99:51–60
46. Baykasoğlu A, Güllü H, Çanakçı H, Özbakır L (2008) Prediction of compressive and tensile strength of limestone via genetic programming. Expert Syst Appl 35(1–2):111–123
47. Cevik A, Akcapınar-Sezer E, Cabalar AF, Gokceoglu C (2011) Modeling of the uniaxial compressive strength of some

clay-bearing rocks using neural network. Appl Soft Comput 11:2587–2594
48. Dehghan S, Sattari Gh, Chehreh Chelgani S, Aliabadi MA (2010) Prediction of uniaxial compressive strength and modulus of elasticity for Travertine samples using regression and artificial neural networks. Min Sci Technol 20:41–46
49. Sarkar K, Tiwary A, Singh TN (2010) Estimation of strength parameters of rock using artificial neural networks. Bull Eng Geol Environ 69:599–606
50. Verma AK, Singh TN (2013) A neuro-fuzzy approach for prediction of longitudinal wave velocity. Neural Comput Appl 22(7–9):1685–1693
51. Singh TN, Verma AK (2012) Comparative analysis of intelligent algorithms to correlate strength and petrographic properties of some schistose rocks. Eng Comput 28:1–12
52. Singh R, Vishal V, Singh TN, Ranjith PG (2012) A comparative study of generalized regression neural network approach and adaptive neuro-fuzzy inference systems for prediction of unconfined compressive strength of rocks. Neural Comput Appl 23(2):499–506
53. Yagiz S, Sezer EA, Gokceoglu C (2012) Artificial neural networks and nonlinear regression techniques to assess the influence of slake durability cycles on the prediction of uniaxial compressive strength and modulus of elasticity for carbonate rocks. Int J Numer Anal Methods 36:1636–1650
54. Meulenkamp F, Grima MA (1999) Application of neural networks for the prediction of the unconfined compressive strength (UCS) from Equotip hardness. Int J Rock Mech Min Sci 36(1):29–39
55. Zorlu K, Gokceoglu C, Ocakoglu F, Nefeslioglu HA, Acikalin S (2008) Prediction of uniaxial compressive strength of sandstones using petrography-based models. Eng Geol 96(3–4):141–158
56. Yilmaz I, Yuksek G (2009) Prediction of the strength and elasticity modulus of gypsum using multiple regression, ANN, and ANFIS models. Int J Rock Mech Min Sci 46(4):803–810
57. Rabbani E, Sharif F, Koolivand Salooki M, Moradzadeh A (2012) Application of neural network technique for prediction of uniaxial compressive strength using reservoir formation properties. Int J Rock Mech Min Sci 56:100–111
58. Rezaei M, Majdi A, Monjezi M (2012) An intelligent approach to predict unconfined compressive strength of rock surrounding access tunnels in longwall coal mining. Neural Comput Appl 24(1):233–241
59. Ceryan N, Okkan U, Kesimal A (2012) Prediction of unconfined compressive strength of carbonate rocks using artificial neural networks. Environ Earth Sci 68(3):807–819
60. Beiki M, Majdi A, Givshad AD (2013) Application of genetic programming to predict the uniaxial compressive strength and elastic modulus of carbonate rocks. Int J Rock Mech Min Sci 63:159–169
61. Mishra DA, Basu A (2013) Estimation of uniaxial compressive strength of rock materials by index tests using regression analysis and fuzzy inference system. Eng Geol 160:54–68
62. Torabi-Kaveh M, Naseri F, Saneie S, Sarshari B (2014) Application of artificial neural networks and multivariate statistics to predict UCS and E using physical properties of Asmari limestones. Arab J Geosci. doi:10.1007/s12517-014-1331-0
63. Momeni E, Jahed Armaghani D, Hajihassani M, Amin MFM (2015) Prediction of uniaxial compressive strength of rock samples using hybrid particle swarm optimization-based artificial neural networks. Measurement 60:50–63
64. ISRM (2007) The complete ISRM suggested methods for rock characterization, testing and monitoring: 1974–2006. In: Ulusay R, Hudson JA (eds) Suggested methods prepared by the commission on testing methods, international society for rock-mechanics. ISRM Turkish National Group, Ankara, Turkey
65. Yagiz S, Gokceoglu C, Sezer E, Iplikci S (2009) Application of two non-linear prediction tools to the estimation of tunnel boring machine performance. Eng Appl Artif Intell 22(4):808–814
66. Yagiz S, Gokceoglu C (2010) Application of fuzzy inference system and nonlinear regression models for predicting rock brittleness. Expert Sys Appl 37(3):2265–2272
67. SPSS Inc (2007) SPSS for Windows (Version 160). SPSS Inc, Chicago
68. Swingler K (1996) Applying neural networks: a practical guide. Academic Press, New York
69. Looney CG (1996) Advances in feed-forward neural networks: demystifying knowledge acquiring black boxes. IEEE Trans Knowl Data Eng 8(2):211–226
70. Nelson M, Illingworth WT (1990) A practical guide to neural nets. Addison-Wesley, Reading
71. Simpson PK (1990) Artificial neural system: foundation, paradigms, applications and implementations. Pergamon, New York
72. Shahin MA, Maier HR, Jaksa MB (2002) Predicting settlement of shallow foundations using neural networks. J Geotech Geoenviron Eng 128(9):785–793
73. Haykin S (1999) Neural networks, 2nd edn. Prentice-Hall, Englewood Cliffs
74. Du KL, Lai AKY, Cheng KKM, Swamy MNS (2002) Neural methods for antenna array signal processing: a review. Signal Process 82:547–561
75. Kalinli A, Acar MC, Gunduz Z (2011) New approaches to determine the ultimate bearing capacity of shallow foundations based on artificial neural networks and ant colony optimization. Eng Geol 117:29–38
76. Kuo RJ, Wang YC, Tien FC (2010) Integration of artificial neural network and MADA methods for green supplier selection. J Clean Prod 18(12):1161–1170
77. Fausett LV (1994) Fundamentals of neural networks: architecture, algorithms and applications. Prentice-Hall, Englewood Cliffs
78. Engelbrecht AP (2007) Computational intelligence: an introduction. Wiley, New York
79. Choobbasti AJ, Farrokhzad F, Barari A (2009) Prediction of slope stability using artificial neural network (case study: Noabad, Mazandaran, Iran). Arab J Geosci 2(4):311–319
80. Erzin Y, Cetin T (2013) The prediction of the critical factor of safety of homogeneous finite slopes using neural networks and multiple regressions. Comput Geosci 51:305–313
81. Momeni E, Nazir R, Jahed Armaghani D, Maizir H (2014) Prediction of pile bearing capacity using a hybrid genetic algorithm-based ANN. Measurement 57:122–131
82. Negnevitsky M (2002) Artificial intelligence: a guide to intelligent systems. Addison-Wesley, England
83. Hassoun MH (1995) Fundamentals of artificial neural networks. MIT Press, Cambridge
84. Fu L (1995) Neural networks in computer intelligence. McGraw-Hill, New York
85. Wyhthoff BJ (1993) Backpropagation neural networks: a tutorial. Chemom Intell Lab Syst 18:115–155
86. Henseler J (1995) Backpropagation. In: Braspenning PJ et al (eds) Artificial neural networks, an introduction to ANN theory and practice., Lecture notes in computer scienceSpringer, Berlin, pp 37–66
87. Hush DR (1989) Classification with neural networks: a performance analysis. In: Proceedings of the IEEE international conference on systems engineering, Dayton, OH, USA, pp 277–280
88. Kanellopoulas I, Wilkinson GG (1997) Strategies and best practice for neural network image classification. Int J Remote Sens 18:711–725

89. Hecht-Nielsen R (1987) Kolmogorov's mapping neural network existence theorem. In: Proceedings of the first IEEE international conference on neural networks, San Diego, CA, USA, pp 11–14
90. Hornik K, Stinchcombe M, White H (1989) Multilayer feedforward networks are universal approximators. Neural Netw 2:359–366
91. Baheer I (2000) Selection of methodology for modeling hysteresis behavior of soils using neural networks. J Comput Aid Civil Infrastruct Eng 5(6):445–463
92. Hajihassani M, Jahed Armaghani D, Sohaei H, Mohamad ET, Marto A (2014) Prediction of airblast-overpressure induced by blasting using a hybrid artificial neural network and particle swarm optimization. Appl Acoust 80:57–67
93. Jahed Armaghani D, Hajihassani M, Mohamad ET, Marto A, Noorani SA (2014) Blasting-induced flyrock and ground vibration prediction through an expert artificial neural network based on particle swarm optimization. Arab J Geosci 7:5383–5396
94. Sonmez H, Gokceoglu C (2008) Discussion on the paper by H. Gullu and E. Ercelebi, "A neural network approach for attenuation relationships: an application using strong ground motion data from Turkey. Eng Geol 97:91–93
95. Ripley BD (1993) Statistical aspects of neural networks. In: Barndoff-Neilsen OE, Jensen JL, Kendall WS (eds) Networks and chaos-statistical and probabilistic aspects. Chapman & Hall, London, pp 40–123
96. Paola JD (1994) Neural network classification of multispectral imagery. MSc thesis, The University of Arizona, USA
97. Wang C (1994) A theory of generalization in learning machines with neural application. PhD thesis, The University of Pennsylvania, USA
98. Masters T (1994) Practical neural network recipes in C++. Academic Press, Boston
99. Kaastra I, Boyd M (1996) Designing a neural network for forecasting financial and economic time series. Neurocomputing 10:215–236
100. Jang RJS (1993) ANFIS: adaptive-network-based fuzzy inference system. IEEE Trans Syst Man Cybern 23:665–685
101. Jang RJS, Sun CT, Mizutani E (1997) Neuro-fuzzy and soft computing. Prentice-Hall, Upper Saddle River
102. Demuth H, Beale M, Hagan M (2009) MATLAB Version 7.14.0.739; Neural network toolbox for use with Matlab. The Mathworks